Supporting Information

A strategy to construct uniform MOFs/PAN nanowires derived bead-like Co_3O_4 for VOCs catalytic combustion

Weigao Han[a,b], Fang Dong[a], Weiliang Han[a], Zhicheng Tang[a*]

(a. State Key Laboratory for Oxo Synthesis and Selective Oxidation, National Engineering Research Center for Fine Petrochemical Intermediates, Lanzhou Institute of Chemical Physics, Chinese Academy of Sciences, Lanzhou 730000, PR China

b. University of Chinese Academy of Sciences, Beijing 100049, PR China)

Experimental section

Chemical and materials. PAN (average Mw 150,000) and 2-methylimidazole (cas 693-98-1) were purchased from Aladdin.

Preparation of H-PAN and NH-PAN 1.8 g of PAN was dissolved into 20 ml DMF. Then nanowires were prepared by the technique of electro-spinning. The feed rate was 1.0 $mL\cdot h^{-1}$. The voltage was 20 V. 0.2 g of the obtained nanowires was put into dilute nitric acid solution. The nanowires need to be teared into thin layers. And it's important to have a good dispersion. The dilute nitric acid solution was made by adding 18 ml into 20 ml nitric acid (ω=65-68%).The temperature was rised up to 80 ^{o}C and kept for 11h. Then the H-PAN was obtained. The obtain H-PAN was flexible not rigidity. The obtained H-PAN was washed with water and was impregnated into 50 ml ammonia for 12h. Then the NH-PAN was obtained. The obtained NH-PAN was washed several times with water.

Preparation of PAN-ZIF, ZIF/H-PAN and ZIF/NH-PAN 2.86 g of $Co(NO_3)_2\cdot 6H_2O$ was dissolved into 100 ml anhydrous methanol. Then the untreated PAN was kept into the solution for 12h. 6.86 g of 2-methylimidazole was dissolved into 100 ml anhydrous methanol. Then the former solution was poured into the latter solution. Then the mixed solution was kept for 24h at 25 ^{o}C. The obtained PAN-ZIF was washed with water under a high stirring speed and dried at room temperature. The ZIF/H-PAN and ZIF/NH-PAN was prepared by the same way except that the untreated PAN was replaced by the H-PAN and NH-PAN.

Preparation of H-Co_3O_4 and NH-Co_3O_4 The H-Co_3O_4 and NH-Co_3O_4 were prepared by thermal treatment of H-PAN and NH-PAN, respectively. The samples were heated at 400 ^{o}C for 1h with a heating rate of 5 ^{o}C min^{-1} in air.

Preparation of Co_3O_4 The Co_3O_4 were prepared by thermal treatment of $Co(NO_3)_2\cdot 6H_2O$. The samples were heated at 400 ^{o}C for 1h with a heating rate of 5 ^{o}C min^{-1} in air.

Characterization of materials

The morphology of the samples was evaluated with transmission electron microscope (TEM). The images of TEM and selected-area electron diffraction patterns were obtained under a microscope of 200 kV using FEI TECNAIG□. Power X-ray diffraction (XRD) analysis was finished at 60 kV and 55 mA with a scanning speed of 0.5° min^{-1}. The 2θ of wide-angle ranged from 10° to 80°. Raman scattering was done by using a Laboratory Human Resources Evolution Raman spectrometer (BX41). The XPS measurement was done on a VG ESCALAB 210 Electron Spectrometer (Mg Kα radiation; hν = 1253.6 eV). The specific surface area and the average pore diameter of the catalysts were measured by nitrogen adsorption with a micromeritics ASAP2010 instrument.

For H_2-TPR, a 40 mg sample was pre-treated at an atmosphere of nitrogen. The temperature was increased from room temperature to 350 °C with a heating rate of 10 °C min^{-1}. When it cooled down to room temperature, the temperature was increased from room temperature to 900 °C with a heating rate of 10 °C min^{-1}. A reducing gas of 5 % vol. H_2 and 95 % vol. N_2 was passed on the sample at the same time.

For O_2-TPD, an 80 mg sample was pre-treated at an atmosphere of nitrogen. The temperature was increased from room temperature to 350 °C with a heating rate of 10 °C min^{-1}. And it was treated for 90 min. When it cooled down to room temperature, the temperature was increased from room temperature to 30 °C for 60 min with a gas of 5 % vol. O_2 and 95 % vol. N_2 passing through. Finally, the temperature was increased from room temperature to 900 °C with a heating rate of 10 °C min^{-1}.

For NH_3-TPD, an 80 mg sample was pre-treated at an atmosphere of nitrogen. The temperature was increased from room temperature to 350 °C with a heating rate of 10 °C min^{-1}. And it was treated for 90 min. When it cooled down to room temperature, the temperature was increased from room temperature to 50 °C for 60 min with a gas of 5 % vol. NH_3 and 95 % vol. N_2 passing through. Finally, the temperature was increased from room temperature to 900 °C with a heating rate of 10 °C min^{-1}.

Catalytic activity measurements

The catalytic oxidation of toluene was evaluated by using a fixed-bed flow reactor operating at steady-state flow mode. Then, 0.4 g catalysts (40-60 mesh) and 0.7 g quartz sand (40-60 mesh) were mixed uniformly. They were put onto the reactor. The reaction gas containing VOCs (3000 ppm) was generated by bubbling air through a VOC saturator, and then passed through the reactor with a weight hourly space velocity (WHSV) of 30000 mL g^{-1} h^{-1}. The first temperature was 100 °C. The activity was measured per 20 °C. Before each test, it needed to stabilize for 2 h. Reactants and products were analyzed with an online GC-6820 gas chromatograph with a flame ionization detector, Conversion was defined as:

$$C_{toluene} = \frac{[C]_{inlet} - [C]_{outlet}}{[C]_{inlet}} \times 100\%$$

The calcination of activation energy

It was reasonable to assume that the oxidation of toluene in the presence of excessive oxygen would follow first-order reaction mechanism. It's respected to toluene concentration:

$$r = -kc = \left(-A\, exp\left(\frac{-Ea}{RT} \right) \right) c$$

Where r, k, A, c and Ea stand for the reaction rate (mol s^{-1}), rate constant (s^{-1}), pre-exponential factor, concentration of toluene in feed stream (mol m^{-3}) and apparent activation energy (kJ mol^{-1}), respectively.

$$r = \frac{F}{W}\left(-ln(1-x)\right)$$

Where F stands for toluene feeding rate (1.08×10^{-7} mol s^{-1}), W stands for the weight of the catalyst (0.4 g), x stands for the toluene conversion. So the equation can be rewritten to:

$$ln\, r = \frac{-Ea}{RT} + B$$

At here, B is a constant. Therefore, the activation energy could be evaluated from the slope of linear ln r versus 1000/T.

The calcination of TOF

$$TOF = \frac{(Pv/RT)\eta}{m_{\mathrm{cat}}\omega\mathrm{Co}/\mathrm{M}_{\mathrm{Co}}}$$

Where P = 0.101 MPa, v is the flow rate of toluene (ml min^{-1}), R = 8.314 J mol^{-1} K^{-1}, η is the toluene conversion (%), m_{cat} is the mass of catalyst (0.4 g), ωCo is the Co loading calculated according to the XPS data (%) and M_{Co} is the molar mass (58.93 g mol^{-1}).

Table S1 Data of characterization of the H-Co_3O_4 and NH-Co_3O_4 samples.

Samples	S_{BET} (m^2/g)[a]	Pore volume/ m^3 g^{-1}	Co^{3+}/Co^{2+}	$O_\beta/(O_\alpha+O_\beta+O_\gamma)$
H-Co_3O_4	39.86	0.17	0.56	0.42
NH-Co_3O_4	31.62	0.15	1.58	0.26

Table S2 Surface area of the H-Co_3O_4 and NH-Co_3O_4 fitted O_2-TPD samples.

Samples	α	α’	β
H-Co_3O_4	425.25	430.01	594.16
NH-Co_3O_4	210.12	368.97	251.69

Table S3 Comparison of different catalysts on the activity of toluene oxidation.

Samples	VOC type	VOC conc. (ppm)	WHSV (mL g^{-1} h^{-1})	T_{90}/℃	Ref. no.
Hollow Co_3O_4	Toluene	3000	30000	246	1
Pd/InOx@CoO_x	Toluene	3000	30000	253	2
Co-CO_3	Toluene	1000	40000	250	3
6.5Au/Fe_2O_3	Toluene	1000	20000	260	4
Mn-Co (1:1)	Toluene	1000	30000	249	5
Bead-like Co_3O_4	Toluene	1000	30000	210	This work

In Table S3, we compared the catalytic performance of our samples with the previous reports. Zhao et al. [1] prepared the hollow Co_3O_4 catalyst derived from ZIF-67, T_{90} of which was 246 ℃. Compared with this, the bead-like Co_3O_4 catalyst showed a better catalytic performance. It might illustrate that the tube-like structure's advantage. Du et al. [2] prepared the tube-like Pd/InOx@CoO_x catalyst derived from Pd/In@ZIF-67, T_{90} of which was 253 ℃. It might turn out that the way that we prepared the catalyst was better than the traditional way. Zhang et al. [3] prepared the nanocrystalline Co_3O_4 catalyst via various precipitants. And different Co_3O_4 catalysts derived from different precipitants had big differences in activity. Compared with the traditional ways, our catalyst also had a good catalytic performance. Han et al. [4] prepared nanodisk-like 6.5Au/Fe_2O_3 catalyst, T_{90} of which was 260 ℃. Qu et al. [5] prepared bimetal Co/Mn catalyst, T_{90} of which was 249 ℃. Compared with bimetal catalyst and other metal catalyst, the bead-like catalyst showed a better catalytic performance.

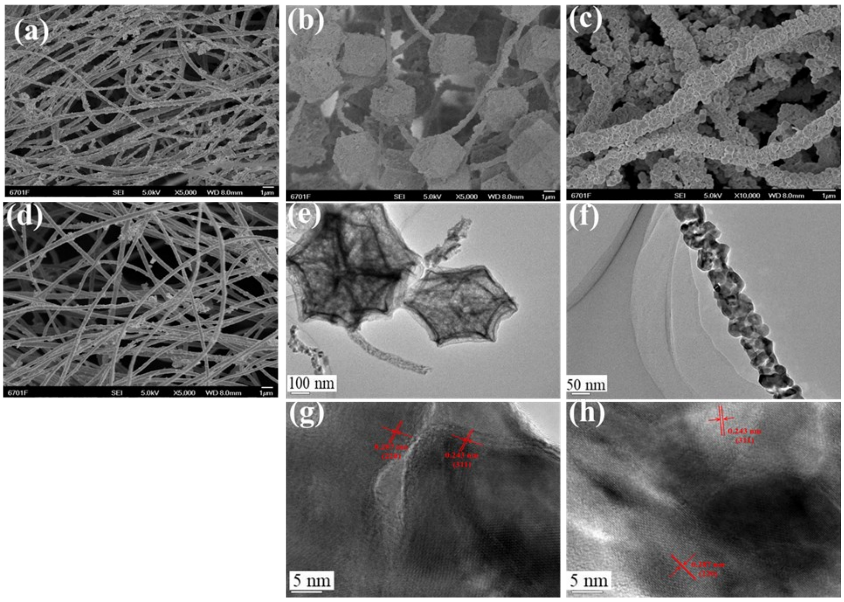

Fig. S1 SEM images of the PAN-ZIF (a) (d), ZIF/H-PAN (b) and ZIF/NH-PAN (c) samples, TEM images of the H-Co_3O_4 (e) and NH-Co_3O_4 (f) samples, HRTEM images of the H-Co_3O_4 (g) and NH-Co_3O_4 (h) samples.

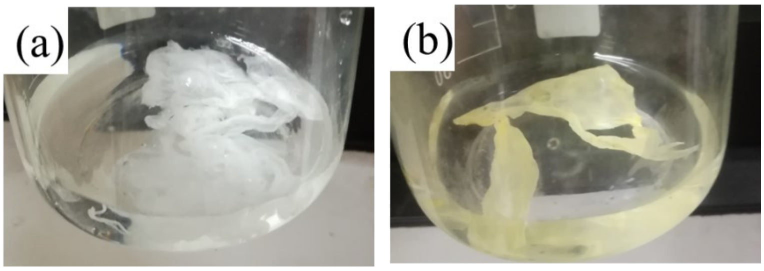

Fig. S2 The image of H-PAN (a), NH-PAN (b).

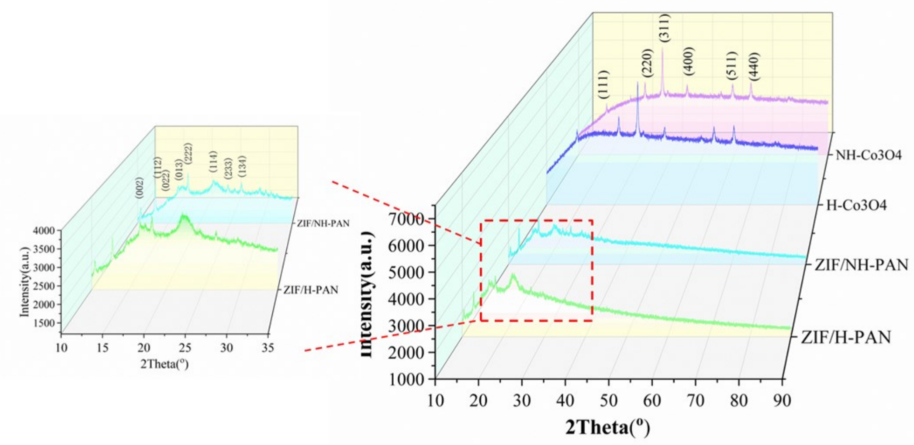

Fig. S3 XRD patterns of the ZIF/H-PAN, ZIF/NH-PAN, H-Co_3O_4 and NH-Co_3O_4 samples.

Fig. S3 showed the XRD patterns of ZIF/H-PAN, ZIF/NH-PAN, H-Co_3O_4 and NH-Co_3O_4. Both of the ZIF/H-PAN and ZIF/NH-PAN showed the same crystal plane of ZIF-67, which was accordance with what reported in other literatures [6]. Peaks at 2θ values of 10.40° (002), 12.73° (112), 14.69° (022), 16.45° (013), 18.03° (222), 22.12° (114), 24.49° (233) and 26.65° (134) were assigned to crystalline ZIF-67. From the XRD result, we could also confirm that ZIF-67 was successfully loaded on the substrate. Peaks of H-Co_3O_4 and NH-Co_3O_4 at 2θ values of 19.00° (111), 31.27° (220), 36.85° (311), 44.80° (400), 59.36° (511) and 65.24° (440) were assigned to crystalline Co_3O_4. Based on the analysis of the half width of the representative diffraction peak for (311), we calculated the crystals' size of both H-Co_3O_4 and NH-Co_3O_4 samples. The crystals' size of H-Co_3O_4 was 24.8 nm and NH-Co_3O_4 was 23.1 nm. The crystals' size of both two samples was almost the same.

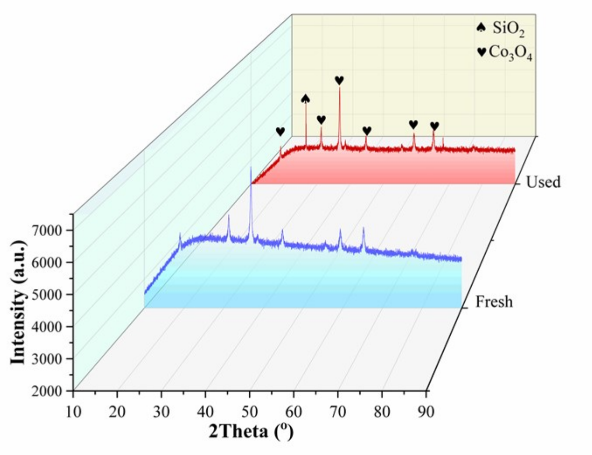

Fig. S4 XRD patterns of the fresh and used H-Co_3O_4 samples.

Fig. S4 showed XRD patterns of the fresh and used H-Co_3O_4 samples. As shown in Fig. S4, both the fresh and used samples showed the same lattice planes of Co_3O_4. It might turn out that the H-Co_3O_4 samples didn’t have an obvious change in phase composition, which might illustrate that the catalyst had a good stability. Peaks at 26.24^o could be assigned to the (011) lattice planes of SiO_2 (PDF-#47-1144). It might be caused by quartz sand, which was mixed with catalyst before they were put into reactor.

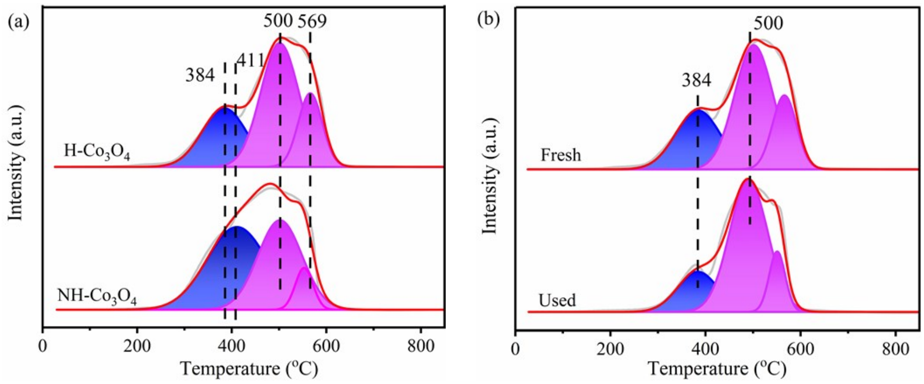

Fig. S5 H_2-TPR curves of the H-Co_3O_4 and NH-Co_3O_4 samples (a), the fresh and used H-Co_3O_4 samples (b).

H_2-TPR was tested to explore the reducibility of the samples. As shown in Fig. S5, both catalysts showed two main peaks. The early peaks at around 400 °C were assigned to the reduction of Co^{3+} to Co^{2+}. Peaks at around 500 °C were assigned to the reduction of Co^{2+} to Co^0 [7]. To prove the stability of the catalyst, the materials after reaction were tested. As shown in Fig. S5, both fresh and used samples showed similar peak position and intensity. It might turn out that the used samples could still keep a good reducibility after a 24 hours' thermal stability test.

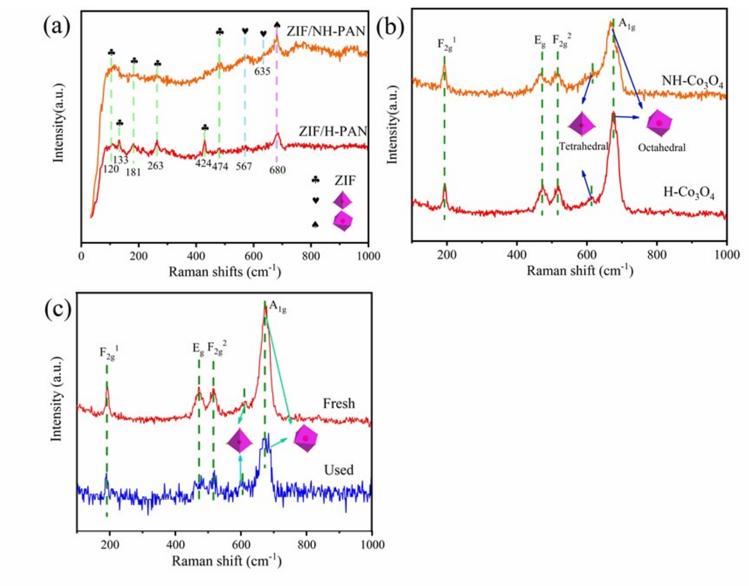

Fig. S6 Raman spectra of the H-PAN, NH-PAN (a), H-Co_3O_4, NH-Co_3O_4 (b) and the fresh and used H-Co_3O_4 (c) samples.

Peak around 120 cm^{-1} could be regarded as vibration of ZIFs' Co ions. Peak at 133 cm$^{-1,}$ 181 cm^{-1}, 263 cm^{-1}, 424 cm^{-1} and 474 cm^{-1} were attributed to ZIFs. As shown in Fig. S6c, There was no blue and red shift of Co-O band. It turned out that the chemical environment of Co didn't have an obvious change after the reaction, which might illustrate that catalyst had a good stability.

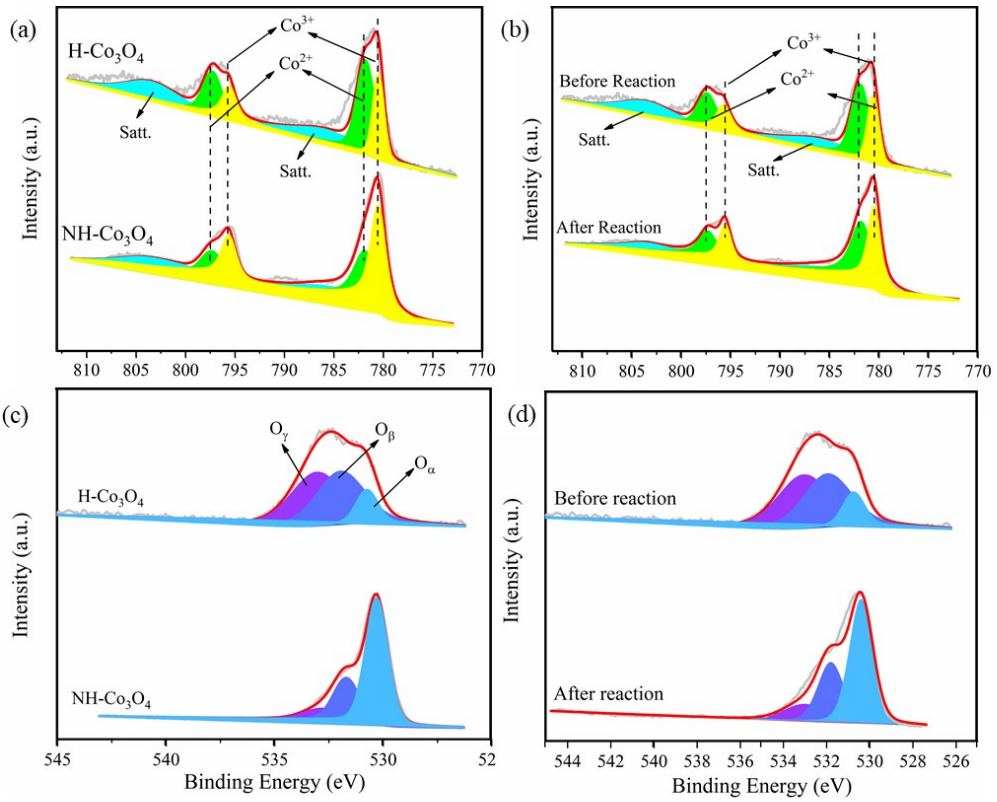

Fig. S7 XPS spectra of the H-Co$_3$O$_4$ and NH-Co$_3$O$_4$ Co 2p (a) samples, the H-Co$_3$O$_4$ samples before and after recation Co 2p samples (b), the H-Co$_3$O$_4$ and NH-Co$_3$O$_4$ O 1s samples (c), the H-Co$_3$O$_4$ samples before and after recation O 1s samples (d).

The peaks of Co 2p were divided into four parts (two main peaks: Co^{3+} and Co^{2+}, and two satellite peaks: Sa1 and Sa2) based on this report [8, 9]. The peaks of O 1s were also divided into lattice oxygen (O$_\alpha$), surface absorbed oxygen (O$_\beta$) and molecular water or hydroxyl groups (O$_\gamma$) [10, 11].

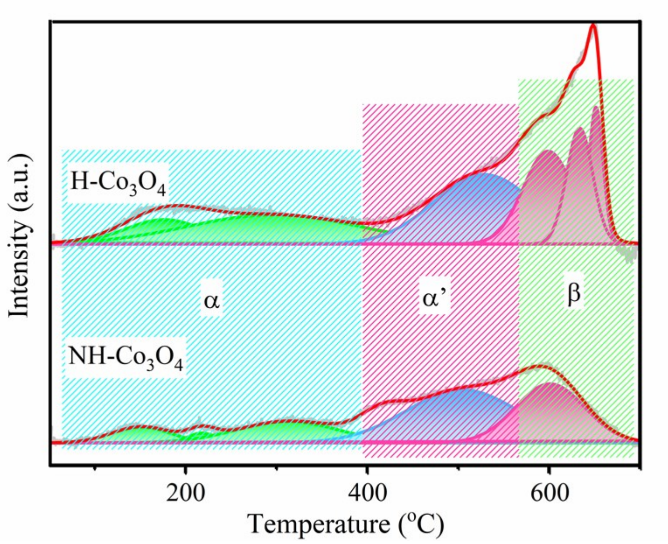

Fig. S8 O_2-TPD curves of the H-Co_3O_4 and NH-Co_3O_4 samples.

O_2-TPD was tested to study the type of oxygen species fatherly. Peaks below 400 °C were considered to weakly chemisorbed oxygen species (α), which was mainly absorbed at surface oxygen vacancies [12, 13]. Peaks between 400 and 600 °C were considered to surface lattice oxygen speices (α'), which was mainly absorbed at lattice defects. Peaks above 600 °C were considered to lattice oxygen (β).

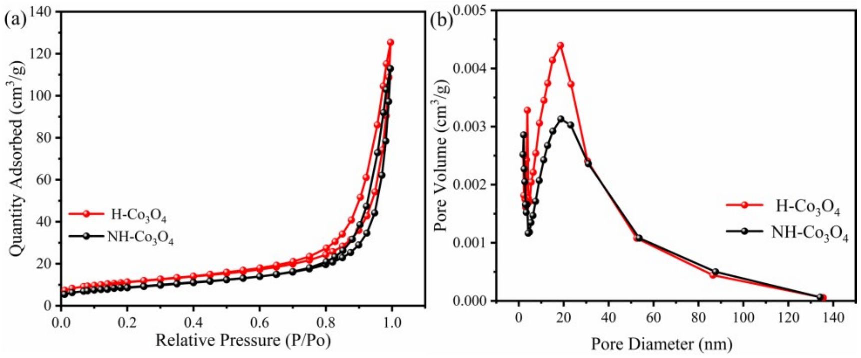

Fig. S9 Adsorption-desorption curves (a) and pore-size distributions (b) of the H-Co_3O_4 and NH-Co_3O_4 samples

Fig. S9a exhibited that both samples exhibited the type Ⅳ H3 at a relatively high pressure. The specific surface areas, pore volumes, pore sizes of the samples were summarized in the Table S1. The specific surface areas of H-Co_3O_4 and NH-Co_3O_4 were 39.86 and 31.62 m² g^{-1}, respectively. The pore volumes of H-Co_3O_4 and NH-Co_3O_4 were 0.17 and 0.15 cm^3 g^{-1}, respectively.

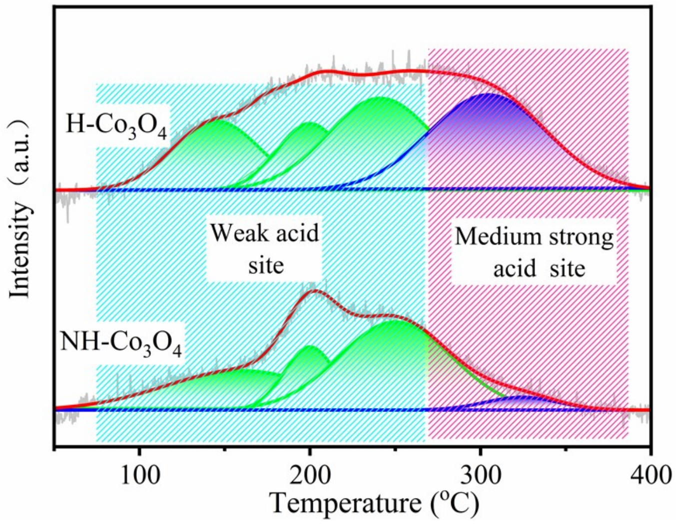

Fig. S10 NH_3-TPD curves of the H-Co_3O_4 and NH-Co_3O_4 samples.

NH_3-TPD was tested to study surface acidity of catalyst. Peaks between 100 and 300 ^{o}C could be regarded as weak acid sites and peaks between 300 and 400 ^{o}C could be regarded as medium strong acid sites [14].

References

1. J. Zhao, Z. Tang, F. Dong, J. Zhang, Mol. Catal., 463 (2019) 77-86.

2. X. Du, F. Dong, Z. Tang, J. Zhang, Nanoscale, 12 (2020) 12133-12145.

3. W. Zhang, J. Dίez-Ramίrezb, P. Anguitaa, C. Descormea, J. Luis Valverdeb, A. Giroir-Fendlera, Appl. Catal. B: Environ., 273 (2020) 118894-118908.

4. W. Han, J. Deng, S. Xie, H. Yang, H. Dai, C. Au, Ind. Eng. Chem. Res., 53 (2014) 3486-3494.

5. Z. Qu, K. Gao, Q. Fu, Y.Qin, Catal. Commun., 52 (2014) 31-35.

6. N. Mahmoodia, M. Taghizadeha, A. Taghizadeha, J. Abdia, B. Hayatib, A. Shekarchi, Appl. Surf. Sci., 480 (2019) 288-299.

7. J. Zhong, Y. Zeng, M. Zhang, W. Feng, D. Xiao, J. Wu, P. Chen, M. Fu, D. Ye, Chem. Eng. J., 397 (2020) 125375-125387.

8. Y. Cao, T. Zi, C. Liu, D. Cui, D. Wu, A. Li, Chem. Comm., 56 (2020) 8675-8678.

9. F. Dong, W. Han, H. Zhao, G. Zhang, Z. Tang, Nanoscale, 11 (2019) 9937-9948.

10. T. Cai, H. Huang, W. Deng, Q. Dai, W. Liu, X. Wang, Appl. Catal. B: Environ., 166-167 (2015) 393-405.

11. J. Zang, S. Wang, F. Wang, Z. Long, F. Mo, Y. Xia, F. Fang, Y. Song, D. Sun, J. Mater. Chem. A, 8 (2020) 14935-14943.

12. X. Weng, W. Wang, Q. Meng, Z. Wu, Catal. Sci. Technol., 8 (2018) 4364-4372.

13. J. Zhang, X. Weng, Z. Wu, Y. Liu, H. Wang, Appl. Catal. B: Environ., 126 (2012) 231-238.

14. L. Zong, G. Zhang, J. Zhao, F. Dong, J. Zhang, Z. Tang, Chem. Eng. J., 343 (2018)

500-511.